

Reaction of hydrogenosilanes with dimethyl Pt(II) complexes promoted by hemilabile P,N-chelating ligands

Susan M. Thompson, Frank Stöhr, Dietmar Sturmayer, Guido Kickelbick, Ulrich Schubert*

Institute of Materials Chemistry, Vienna University of Technology, Getreidemarkt 9, A-1060 Wien, Austria

Received 3 April 2003; received in revised form 24 July 2003; accepted 24 July 2003

Abstract

Reaction of $[(\kappa^2\text{-P,N})\text{-Me}_2\text{N}(\text{CH}_2)_3\text{PPh}_2]\text{PtMe}_2$ $[(\text{P}\cap\text{N})\text{PtMe}_2]$ with HSiR_3 (triethylsilane or diphenylmethylsilane) results in the formation of MeSiR_3 and the methyl silyl complexes $(\text{P}\cap\text{N})\text{Pt}(\text{Me})\text{SiR}_3$. In the early stages of the reaction, the hydrido complex $(\text{P}\cap\text{N})\text{Pt}(\text{Me})\text{H}$ is additionally observed. In the reaction of HSiMePh_2 , the rearranged complex $(\text{P}\cap\text{N})\text{Pt}(\text{Ph})\text{SiMe}_2\text{Ph}$ is also formed. The reactivity of the complexes $(\text{P}\cap\text{N})\text{PtMe}_2$ is influenced by the kind of chelating $\text{P}\cap\text{N}$ ligand and appears to depend on how easily the amino group is de-coordinated.

© 2003 Elsevier B.V. All rights reserved.

Keywords: Hemilabile ligands; Methyl/silyl exchange; Oxidative addition; Metal silyl complexes

1. Introduction

The reactivity of Pt(II) complexes towards organosilanes is greatly enhanced when hemilabile chelating ligands $\text{R}_2\text{N-R}'\text{-PPh}_2$ ($\text{P}\cap\text{N}$) are employed, compared with the corresponding bis(phosphine) complexes, and several new catalytic and stoichiometric reactions have been observed [1]. For example, $\text{P}\cap\text{N}$ -substituted Pt(II) complexes activate both C–Cl and Si–Cl bonds [2] and catalyze the formation of disiloxanes from HSiR_3 [3] and C–Cl/Si–H exchange reactions [4]. The corresponding bis(phosphine) complexes undergo none of these reactions.

A key entry to metal silyl complexes are oxidative addition reactions of hydrogenosilanes. While $(\text{dppe})\text{-PtMe}_2$ (dppe = bis(diphenylphosphino)ethane), for ex-

ample, does not react with HSiR_3 at ambient conditions, $(\text{P}\cap\text{N})\text{PtMe}_2$ readily reacts with trimethoxysilane [5] (Eq. (1a)) or 1,2-bis(dimethylsilyl)benzene [6] (Eq. (1b)). Reaction with the latter silane yielded the corresponding chelated bis(silyl) complex. Noteworthy was the fact that for the complete reaction of the dimethyl complexes two equivalents of 1,2-bis(dimethylsilyl)benzene must be employed. While one equivalent of the silane is necessary to form the bis(silyl) ligand, the second equivalent turns up as 1-dimethylsilyl-2-trimethylsilyl-benzene, i.e. one methyl ligand of the starting complex is eliminated as the methylsilane and the other as methane. The formation of the corresponding bis(silyl) complex and methylsilane was also observed in the reaction of $[(\kappa^2\text{-P,N})\text{-Me}_2\text{NCH}_2\text{CH}_2\text{PPh}_2]\text{PtMe}_2$ with $\text{HSi}(\text{OMe})_3$, but the reaction was more complex: (i) only about half of the starting complex was converted to the bis(silyl) complex $(\text{P}\cap\text{N})\text{Pt}[\text{Si}(\text{OMe})_3]_2$, while the remainder turned up as the mono-substituted complex $(\text{P}\cap\text{N})\text{Pt}[\text{Si}(\text{OMe})_3]\text{Me}$. This implies that the first methyl/silyl exchange reaction at the platinum center is

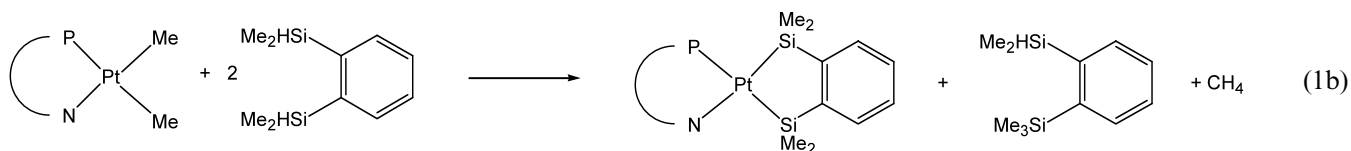
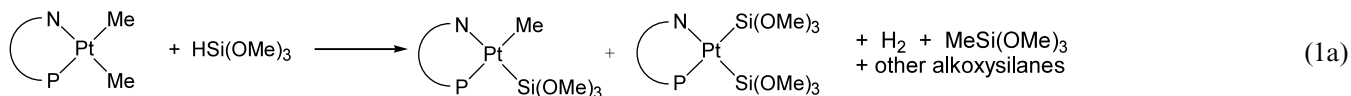
* Corresponding author. Tel.: +43-1-58801-15320; fax: +43-1-58801-15399.

E-mail address: uschuber@mail.zserv.tuwien.ac.at (U. Schubert).

faster than the second: (ii) when an excess of $\text{HSi}(\text{OMe})_3$ was employed, the hydrogenosilane was catalytically converted into $\text{Si}(\text{OMe})_4$.

2.1. Reaction of **1** with HSiEt_3

The first silane investigated was HSiEt_3 (Eq. (2)). On



The reactions of trimethoxysilane and 1,2-bis(dimethylsilyl)benzene were promoted by the high tendency of both silanes towards oxidative addition reactions, due to the activated Si–H bond in the case of $\text{HSi}(\text{OEt})_3$ and the chelate-assistance in the case of 1,2-bis(dimethylsilyl)benzene, respectively. In the work presented in this article, the reactions of $(\text{P} \cap \text{N})\text{PtMe}_2$ (**1**) ($\text{P} \cap \text{N} = \text{Ph}_2\text{P}(\text{CH}_2)_3\text{NMe}_2$) with the less reactive silanes diphenylmethylosilane and triethylsilane were investigated. The course of the reactions was analyzed by multi-nuclear NMR spectroscopy. Since we were mainly interested in elucidating the reaction mechanism, no attempts were made to isolate the products. All reactions were carried out in a poly(tetrafluoroethylene) (PTFE) liner to exclude the possibility of metal catalyzed reactions of the silane with adsorbed water or Si–OH groups on the glass surface [7].

2. Results and discussion

As in the reactions of trimethoxysilane or 1,2-bis(dimethylsilyl)benzene, no reaction was seen between $(\text{PhMe}_2\text{P})_2\text{PtMe}_2$ or $(\text{dppe})_2\text{PtMe}_2$ and HSiEt_3 or HSiMePh_2 . In contrast, when the neat silanes, in various stoichiometric ratios were added to benzene solutions of **1** at room temperature, slight gas evolution was observed, and NMR spectra taken immediately after silane addition indicated an instantaneous start of the reactions.

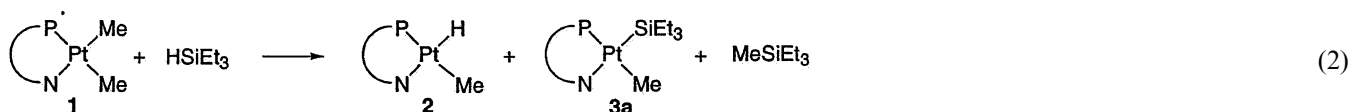
addition of one equivalent of HSiEt_3 to **1** at room temperature, the ^{29}Si -NMR spectrum showed the immediate formation of MeSiEt_3 , and the ^{31}P -NMR spectrum the presence of complex **2** (see below). About 13% of the phosphorous species seen in the NMR spectrum was complex **2**, and the rest was the reactant **1** (compared with an internal standard which did not partake in the reaction) [8]. Complex **2** was only observed during the first hour of reaction.

Only platinum satellites ($^1J_{\text{PtP}} = 2208$ Hz) but no $^2J_{\text{SiPtP}}$ coupling was seen in the ^{31}P -NMR spectrum of **2**, and the chemical shift ($\delta = 14.9$) was very similar to that of **1**. No new ^{29}Si -NMR signal was observed. The platinum-bonded hydrogen was identified in the ^1H -NMR spectrum with the characteristic upfield shift at -18.9 ppm ($^2J_{\text{PH}} = 17$ Hz and $^1J_{\text{PH}} = 1442$). Furthermore, 2D HP-HMBC experiments showed a coupling between this proton and the corresponding phosphorus signal. The intensity of this signal was found to be only approximately one-twentieth of the Si–H proton of unreacted HSiEt_3 after 30 min reaction. The Pt–Me signal could not be identified in the ^{13}C -NMR spectrum due to the many overlapping signals in the relevant region. Because the spectroscopic data of this complex were the same independent of the employed silane (see below), we postulate that **2** is $(\text{P} \cap \text{N})\text{Pt}(\text{H})\text{Me}$. Further evidence is given later in the text. The *cis* arrangement of P and H was also supported by DFT calculations (see below).

A second new complex with a ^{31}P -NMR chemical shift of 23 ppm and typical platinum satellites was first

seen after about 45 min reaction at room temperature and was assigned to the methyl silyl complex (P∩N)Pt(Me)SiEt₃ (**3a**). The stereochemistry of **3a** was confirmed earlier for related complexes [5,9] and can be explained by the different *trans* influence of the nitrogen and phosphorus donor centers.

undergo reaction with a further hydrogenosilane to give the methyl silyl complex **3a** by hydrogen elimination. This mechanistic suggestion is supported by the observation that **2** is only present in approximately the first hour of reaction, after which it was no longer seen (Scheme 1).



After 4 h of reaction, the strongest ³¹P-NMR signal was still that of the reactant complex **1**. Small amounts of de-coordinated P∩N ligand, as well as other phosphorus containing species were also evident besides complex **3a**. At this point, HSiEt₃ was only detected in traces in the ²⁹Si-NMR spectrum. Both complex **1** and the silane were completely consumed after 24 h at room temperature.

The sequence in which the various compounds appeared and disappeared was essentially the same when **1** was reacted with a 20-fold excess of HSiEt₃. Complex **2** and MeSiEt₃ were immediately visible in the NMR spectra. After 4 h of reaction the portion of **2** was slightly higher (23%), and **1** was completely consumed after 16 h. Complex **2** was again only identified in the first hour of reaction. Complex **3a** was first identified within 1 h reaction at room temperature and was present in approximately the same magnitude as **1** after 3.25 h. After 18 h, **3a** was the only platinum complex present. Contrary to the 1:1 reaction, there was no evidence of other phosphorus species. Due to the large excess and our assumption that the reaction is stoichiometric, HSiEt₃ was never completely consumed. After reaction times of longer than 3 h, traces of other silicon species were observed in the ²⁹Si-NMR spectrum besides HSiEt₃ and MeSiEt₃. Because of the large excess of HSiEt₃ the other silicon-containing species were difficult to assign.

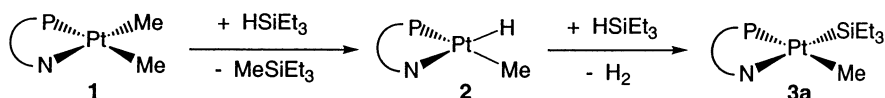
The experimental findings suggest the following reaction mechanism. The incoming silane, with the strongest *trans* effect of all the ligands involved, causes the nitrogen atom of the P∩N ligand to de-coordinate. Elimination of methylsilane would give the observed methyl hydride complex. This complex then could

The proposed reaction pathway was also investigated by DFT calculations. The two reaction steps shown in Scheme 2 (energies in kcal mol⁻¹), i.e. the formation of **2** from **1** and the formation of **3** from **2**, were calculated with the necessary simplifications to give model systems suitable for DFT calculations. Each of the shown structures were optimized, indicating that the structures are stable. The corresponding energies are also given for each step.

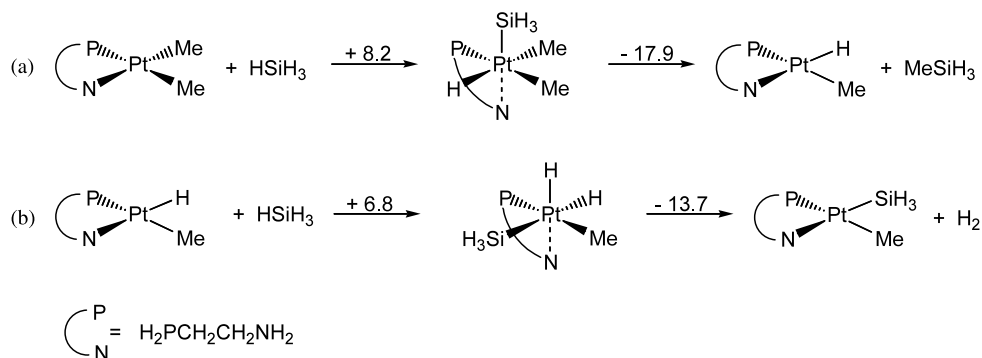
Overall it can be seen that both reactions are exothermic, reaction (a) with -9.7 kcal mol⁻¹, and reaction (b) with -6.9 kcal mol⁻¹. In each case a six-coordinate intermediate was also found and its geometry optimized.

2.2. Reaction of **1** with HSiMePh₂

When an equimolar amount of HSiMePh₂ was added (Eq. (3)), complex **1** was not completely consumed within 30 h of reaction at room temperature, nor with heating for 2 h at 60 °C. The ²⁹Si- and ¹H-NMR spectra showed the immediate formation of the methylsilane, Me₂SiPh₂. The first new platinum complex observed in the ³¹P-NMR spectrum immediately after addition of the silane was again **2**. Complex **2** was only visible for the first hour of the reaction at room temperature. Here again the platinum bonded hydrogen in complex **2** was identified in the ¹H-NMR spectrum (-18.9 ppm), with phosphorus coupling and platinum satellites. The other signal (a doublet at 24 ppm with platinum satellites), also visible in the first ³¹P-NMR spectrum taken after addition of the silane, was assigned to the methyl silyl complex **3b**. The coupling constant of ca. 11 Hz is characteristic for phosphorus silicon coupling, and



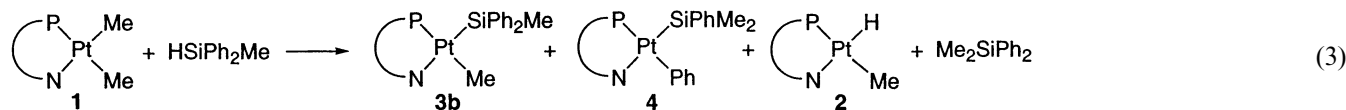
Scheme 1.



Scheme 2.

being a doublet indicates that only one equivalent silicon is present (Fig. 1). The $^1J_{\text{PtP}}$ coupling constant was also within the expected range for such complexes.

after 1 h. Further peaks were clearly identified in the ^{29}Si -NMR spectrum at -10.6 ppm and -21.7 ppm throughout the complete reaction period. These were



However, contrary to the HSiEt_3 reaction, a third new complex (**4**) was also formed. Complex **4**, found at 28 ppm in the ^{31}P -NMR spectrum, also had a doublet with virtually the same coupling constant as **3b**, and platinum satellites with a coupling constant of 1597 Hz. This complex was first observed after 4 h at room temperature while the reactant platinum complex **1**. The spectroscopic data strongly suggest that **4** has the composition and structure as shown in Eq. (3) (see below). Although further smaller unidentified phosphorus peaks were found, no free P,N-chelated ligand was observed. Complexes **3b** and **4** were the only complexes present at the end of the reaction.

Only traces of HSiMePh_2 were seen in the ^1H -NMR spectrum after reaction for 5 h at room temperature. After heating at 60°C the reactant silane had vanished

assigned to the silyl ligands of **3b** and **4**. No clear platinum satellites were visible. However two-dimensional spectra indicated coupling with platinum, and literature values support the assignment.

When **1** and HSiMePh_2 were reacted in a 1:20 ratio, the outcome of the reaction was essentially the same. Me_2SiPh_2 was again formed immediately. The ^{31}P -NMR spectrum showed that **1** was consumed within 15 min reaction at room temperature. Complex **2** was only identified in the first spectrum taken and was consumed within 15 min reaction at room temperature. Both complex **3b** and **4** were seen immediately and still present at the end of the reaction. After 5 h reaction at room temperature, and with additional heating at 60°C , **3b** and **4** were the only phosphorus species present in approximately the same amount. The silane, being used

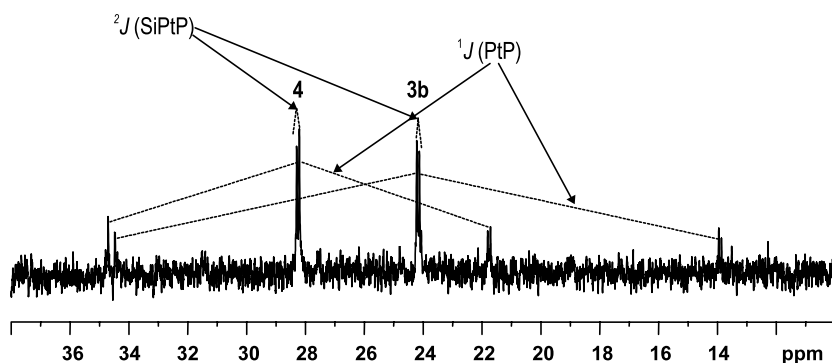


Fig. 1. Section from the ^{31}P -NMR spectrum of the reaction mixture between **1** and HSiMePh_2 (1:20) after 2 h reaction at room temperature.

in excess, was not completely consumed, even after heating for 5 h at 60 °C.

With regard to the identity of complex **4**, it must be emphasized, that due to the complexity of the NMR spectra the exact identity of the silyl group bonded to platinum is not completely certain. We cannot totally rule out that the silyl ligand is SiHPh₂ (though no signal was found in the expected region in the ¹H-NMR spectra) or SiMe₂Ph rather than SiMePh₂. However, as will be discussed in the following paragraph, the mechanistic possibilities leading to SiHPh₂ or SiMe₂Ph are rather unlikely to happen.

There are several possibilities how a complex of the type (P∩N)Pt(Ph)SiR₃ could be formed. Reaction of some intermediate complex with the solvent (benzene) can be ruled out, because no phenyl–silyl complex was observed in the reaction of HSiEt₃. A further possibility is the direct addition of a Si–Ph bond, either of the starting silane HSiMePh₂ or the product silane Me₂–SiPh₂ to some intermediate platinum complex. The first possibility would result in the formation of (P∩N)Pt(Ph)SiHMePh and the second in the formation of (P∩N)Pt(Ph)SiMe₂Ph. Activation of Si–Ph bonds has been observed upon reaction of Ph₂PCH₂CH₂SiPh_{3–n}–Me_n (*n* = 0, 1) with (Ph₃P)₂Pt(π–C₂H₄) [10]. In the same work was shown that the Si–Me bonds were not reactive enough to be added to the platinum center. This would explain why **4** was observed in the reaction of HSiMePh₂, but no analogous complex in the reaction of HSiEt₃. The possibility of a Si–Ph oxidative addition is nevertheless rather unlikely in the present case, because complex **4** is already observed while unreacted HSiPh₃ is still present. Any reactive intermediate capable of oxidative addition reactions would preferentially react with the much more reactive Si–H bonds rather than Si–Ph groups.

The most probable explanation is that **4** is formed by a rearrangement of **3**, i.e. that the composition of the complex is (P∩N)Pt(Ph)SiMePh₂. Scrambling reactions of silicon substituents in metal silyl complexes are not uncommon and are usually explained by the intermediate formation of silylene complexes [11]. Tilley et al. have pointed out that transfer of a substituent from silicon to platinum is easier in a three, rather than four-coordinate complex [12]. Hence such a reaction may be enabled through the presence of the hemilabile ligand. An analogous reaction was also observed in the reaction of HSi(OMe)₃ with P∩N-chelated complexes [5].

2.3. Comparison of the reactivity of the different P,N-chelated platinum complexes

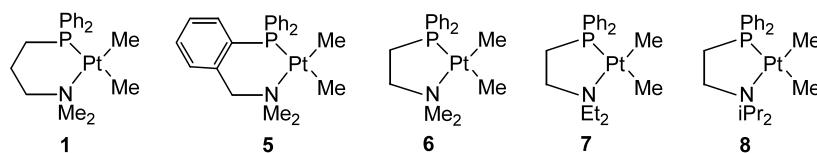
The reaction of HSiMePh₂ was used to test the reactivity of (P∩N)PtMe₂ complexes with different P∩N ligands (Scheme 3). A 20-fold excess of the silane was employed. Though the ³¹P- and ²⁹Si-NMR spectra

cannot be integrated, it was still possible to qualitatively analyze the spectra and compare the consumption of the reactant platinum complex and the formation of the methylsilane.

When comparing the complete consumption of the reactant platinum complex (through the ³¹P-NMR spectra) at room temperature, the order is **8** < **1** < **1** h < **7** < **5** < 13 h < **6**. Comparison of the intensity of the Me₂SiR₂ signal in the ²⁹Si-NMR spectra after 1 h at room temperature gave the following order: **1** > **8** > **7** > **5** ≈ **6**. Both series reflect similar trends and clearly show that the employed P∩N ligand has a significant influence on the reactivity of the complexes. These series also indicate that the formation of the methyl silane is closely related to the consumption of the reactant platinum complex. The P∩N-chelating ligand is thought to enable the reaction between the bis(methyl) complexes and hydrogenosilanes either through the fact that the methyl groups are differently activated, and/or through the chelating ligand's ability to reversibly de-coordinate.

Complexes **1** and **5** have a three carbon chain between the nitrogen and phosphorus donor centers, but the phenyl ring in **5** restricts the flexibility of the ligand. The other complexes, **6**, **7** and **8**, all have ethylene bridges between the donor centers, but vary in the organyl groups at the nitrogen center. From these results it can be seen that the complexes in which the amino group de-coordinates most easily had the fastest reaction rates. In complex **1**, the six-membered ring is less favorable than the five-membered ring in the corresponding complex **6**, and in complex **8** the large *iso*-propyl groups provide some steric hindrance. The stiffening of the chelate ring in **5** results in a less facile de-coordination of the amino group relative to **1**.

This is, to some extent, also reflected in the structural data of the (P∩N)PtMe₂ complexes **1**, **6** and **8** (Table 1 and Figs. 2 and 3). In each case, the Pt–N distance is in the range of the Pt–P distance—or even longer—despite the smaller radius of nitrogen compared to phosphorus. The weak Pt–N interaction results in a strengthening of the Pt–Me bond *trans* to N; the Pt–C bond lengths *trans* to N are distinctly shorter than that *trans* to P. The longest Pt–N distance is found in **8**, probably because of the steric hindrance of the *iso*-propyl groups, while the Pt–N distance in **6** is shortest in this series. An interesting structural feature with regard to the reactivity is the large N–Pt–P angle in **1**, which is more than 10° wider than in the five-membered ring systems **6** and **8**. This distortion might be the reason for the higher reactivity of **1** compared to **6**. However, a word of caution is necessary at this point: The structural variations among the complexes **1**, **6** and **8** are more complex, i.e. the reactivity differences cannot be traced back to a single structural parameter. For example,



Scheme 3.

Table 1

Typical bond lengths (in pm) and angles in complexes (P \cap N)PtMe₂

P \cap N	Ph ₂ PCH ₂ CH ₂ NMe ₂ (6) [6]	Ph ₂ PCH ₂ CH ₂ N ⁱ Pr ₂ (8)	Ph ₂ PCH ₂ CH ₂ CH ₂ NMe ₂ (1)
Pt–C (<i>trans</i> P)	206.9(8)	210.2(6)	210.3(9)
Pt–C (<i>trans</i> N)	203.7(9)	204.5(7)	203.4(10)
Pt–N	221.0(7)	230.2(5)	223.9(8)
Pt–P	224.3(2)	224.6(2)	224.2(2)
N–Pt–P	84.6(1)	84.0(1)	95.5(2)
P–Pt–C (<i>cis</i>)	96.5(2)	93.2(3)	89.4(4)
N–Pt–C (<i>cis</i>)	92.0(2)	96.7(2)	91.0(4)
C–Pt–C	87.0(3)	86.0(3)	84.1(5)

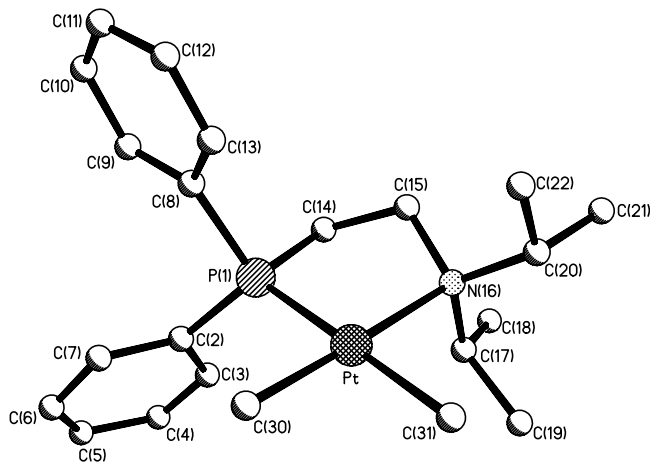
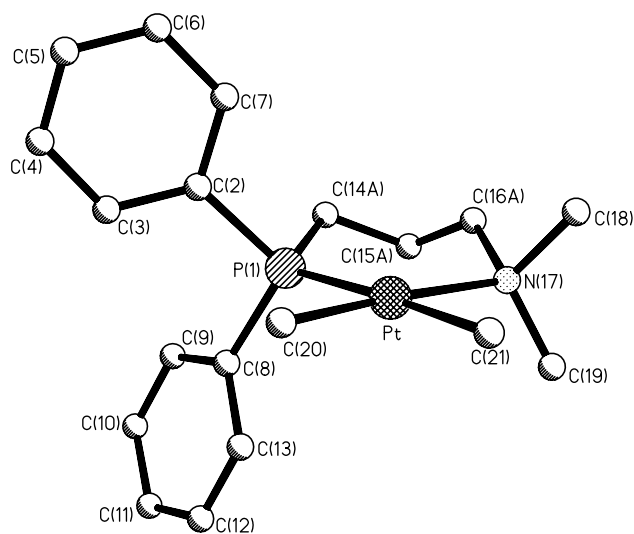
there is no straightforward explanation for the shorter Pt–C (*trans* to P) distance in **6**.

3. Conclusions

The mono-substitution of the platinum complex occurred relatively easily in all cases irrespective of the silane used. The order of reactivity was HSiMePh₂ > HSiEt₃ reflecting the inductive effect of the different substituents at the silicon atom.

In previous work, we had employed trimethoxysilane and 1,2-bis(dimethylsilyl)benzene for the reactions with complexes of the type (P \cap N)PtMe₂. Both silanes have a higher tendency towards oxidative addition reactions than the silanes used in this work, viz. diphenylmethylsilane and triethylsilane. As a result of the lower

reactivity of the latter silanes, substitution of the second methyl ligand of the starting complex was not observed, and the reaction rate of the first step was slowed down. It appears that substitution of the second methyl group requires significantly more energy, therefore it can be inferred that a bis(silyl) complex can only be formed with an incoming silane which is somehow activated, which is not the case for diphenylmethylsilane or triethylsilane. A possible explanation for the lower reaction rate of the second methyl/silyl exchange could be the *trans* effect of the involved ligands. Contrary to the Pt(IV) intermediate for the first step (Scheme 2), the second SiR₃ group in the corresponding intermediate for the second exchange must have a different *trans* ligand.

Fig. 2. Molecular structure of [(κ²-P,N)-Ph₂PCH₂CH₂NⁱPr₂]PtMe₂ (**8**).Fig. 3. Molecular structure of [(κ²-P,N)-Ph₂PCH₂CH₂CH₂NMe₂]PtMe₂ (**1**).

This is obviously less favorable than the exchange of first SiR_3 ligand being *trans* to CH_3 , and therefore the second substitution does not take place for non-activated silanes.

The stabilization of the mono-substituted complex was previously also observed in the reaction of $(\text{P} \cap \text{N})\text{PtMe}_2$ with HSnR_3 ($\text{R} = \text{Bu}, \text{Ph}$), where $(\text{P} \cap \text{N})\text{Pt}(\text{SnR}_3)\text{Me}$ was a major product, along with MeSnR_3 [13]. The main difference between the reaction of the stannanes and the silanes reported here is that stannanes are more reactive. The reaction therefore proceeds by formation of bis(stannyl) complexes and distannanes.

The slower reaction of diphenylmethylsilane and triethylsilane compared with trimethoxysilane, 1,2-bis(dimethylsilyl)benzene and the stannanes allowed us to study the first methyl/silyl exchange step in more detail than was hitherto possible. When analyzing the results obtained for the reaction of **1** with the hydrogenosilanes, it seems that the methyl silyl complexes are formed together with the corresponding methylsilane, i.e. that the first Pt-Me ligand is eliminated as a methylsilane. This is different to what we had previously postulated (methane elimination in the first step) [5]. A strong evidence for the methylsilane-elimination pathway in the reactions of the silanes investigated in the present work, apart from the observed products, is that **1** was never completely consumed in the 1:1 reactions, while the starting hydrogenosilane was. Thus, more than one equivalent of the silane is obviously needed for the formation of the methyl silyl complexes.

Although we did not observe clear gas evolution when **1** and the silanes were reacted in a 1:1 molar ratio, a competing methane elimination cannot be excluded, at least as a minor parallel reaction. A competition between methylsilane and methane elimination from intermediates containing hydrido, alkyl and silyl ligands (and the ratio of both reactions depending on the nature of the silyl group) was already observed for other complexes, such as *mer*-(Me_3P) $_3\text{Ir}(\text{SiR}_3)(\text{H})\text{Me}$ [14] or $(\text{Cp}^*_2\text{ScMe} + \text{MesSiH}_3)$ [15].

If the first methyl/silyl exchange of $(\text{P} \cap \text{N})\text{PtMe}_2$ proceeds by methylsilane elimination, then the second exchange must proceed by methane elimination, because both methane and methylsilane were clearly identified in the experiments with trimethoxysilane and 1,2-bis(dimethylsilyl)benzene (see Eq. (1)) (and because one methyl-silyl group per bis(silyl) complex is formed). This difference between the first and the second exchange step is probably again due to the different *trans* effects in the intermediate $\text{Pt}(\text{IV})$ complexes.

The reactions of HSiMePh_2 with the complexes $(\text{P} \cap \text{N})\text{PtMe}_2$ having different $\text{P} \cap \text{N}$ ligands showed that the proper choice of the $\text{P} \cap \text{N}$ ligand allows to tailor the reactivity of the complexes towards silanes, which could

be particularly important to obtain selectivity in the catalytic reactions previously observed.

4. Experimental

All reactions were carried out using standard Schlenk techniques in an argon atmosphere. Argon was purified using Cu and molecular sieve (4 Å). All solvents used were dried and distilled at least once under argon. All NMR measurements were carried out in deuterated benzene (C_6D_6), the samples were filled and sealed in an argon atmosphere. Benzene- d_6 was pre-dried using a molecular sieve (4 Å) and then made oxygen-free using the freeze-pump-thaw method. The reactions were carried out in a poly(*tetra*-fluoroethylene) (PTFE) liner to exclude the possibility of metal catalyzed reactions of the silane with adsorbed water or Si-OH groups of the glass surface. Reactions were also carried out directly in glass vessels, the results obtained here were as seen with the use of a PTFE liner, but siloxane species were also present.

The complexes $(\text{P} \cap \text{N})\text{PtMe}_2$ were prepared by the previously described general procedure [6].

NMR experiments were taken on Bruker Avance 300 and 250 MHz spectrometers at room temperature (r.t.), unless otherwise stated, using an external standard; TMS, 85% H_3PO_4 or $\text{Na}_2\text{Pt}(\text{H}_2\text{O})_6$, for ^1H -, ^{31}P - and ^{195}Pt -NMR, respectively. All pulse programs used were obtained from the standard Bruker software library. ^{31}P -, ^{195}Pt - and ^{13}C -NMR spectra were proton decoupled, ^{29}Si was measured using a INEPT sequence, or through 2D $^1\text{H}^{29}\text{Si}$ correlation technique HMBC. Further 2D experiments were performed using a HMBC technique for $^1\text{H}^{31}\text{P}$ and $^1\text{H}^{195}\text{Pt}$ correlations to aid peak assignments. Although ^{13}C -NMR spectra were also taken, these data are not reported here, because the spectra are very complex and do not allow an unequivocal assignment of the peaks.

The NMR signals seen throughout the course of the reaction are given in the following paragraphs, including those which are only seen at specific reaction times. Further specific information is given in the main text. For these reasons chemical shifts are given without integration, as this varies throughout the course of the reaction. For clarity, the key NMR data are summarized in Table 2.

4.1. Computational details

The geometry optimizations of the equilibrium geometries and transition structures were performed using the B3LYP version of DFT, which is comprised of Becke's hybrid three-parameter exchange functional and the correlation functional of Becke, Lee and co-workers [16,17]. The LanL2DZ basis set implemented in the

Table 2
Summary of relevant NMR data

Complex/silane	δ (^{31}P)	δ (^{29}Si)	δ (^1H) H–Si or H–Pt
1	15.23 ($^1J_{\text{PtP}} = 2089$ Hz)	–	–
2	14.91 ($^1J_{\text{PtP}} = 2208$ Hz)	–	–18.22 ($^2J_{\text{PH}} = 17$ Hz, $^1J_{\text{PtH}} = 1442$ Hz)
3a	23.04 ($^1J_{\text{PtP}} = 2850$ Hz)	15.7	–
3b	24.17 ($^2J_{\text{SiPtP}} = 10.7$ Hz, $^1J_{\text{PtP}} = 2494$ Hz)	–10.6	–
4	28.23 ($^2J_{\text{SiPtP}} = 10.7$ Hz, $^1J_{\text{PtP}} = 1597$ Hz)	–21.6	–
HSiEt ₃	–	0.05	3.98 ($^2J_{\text{SiCH}} = 4$ Hz, $^1J_{\text{SiH}} = 35$ Hz)
MeSiEt ₃	–	6.6	–
HSiPh ₂ Me	–	–17.7	4.94 ($^2J_{\text{SiCH}} = 4\text{Hz}$, $^1J_{\text{SiH}} = 41$ Hz)
MeSiPh ₂ Me	–	7.97	–

GAUSSIAN-98 package [18], was used an all atoms for the calculations. Vibrational mode analyses were carried out to confirm that on potential energy surfaces optimized geometries correspond to a local minimum without an imaginary frequency mode or a saddle point with only one imaginary mode. Corrections of zero-point vibrational energies were taken into account in stationary structures obtained. All of the calculations were carried out with the GAUSSIAN-98 package of electronic structure programs [18].

4.2. Reaction of $[(\kappa^2\text{-P,N})\text{-Me}_2\text{N}(\text{CH}_2)_3\text{PPh}_2]\text{PtMe}_2$ (**1**) with HSiEt₃

1:1 molar ratio: 3.04 mg (0.03 mmol) of HSiEt₃ was added at r.t. to 13 mg (0.03 mmol) of **1** in 0.5 ml of C₆D₆. On addition of the silane the reaction mixture turned yellow. With increasing reaction time the sample became darker in color, and after 24 h at r.t. the sample was dark brown.

Excess of silane: 56 mg (0.48 mmol) of HSiEt₃ was added at r.t. to 12 mg (0.02 mmol) of **1** in 0.5 ml of C₆D₆. On addition of the silane, gas evolution was observed and the sample turned yellow. After 2 h at r.t. the sample was orange/brown, with some brown solid.

$^1\text{H-NMR}$: $\delta = -18.22$, (d with satellites, $^2J_{\text{PH}} = 17$ Hz, $^1J_{\text{PtH}} = 1442$ Hz, **2**), 3.98 (quin, with satellites, $^2J_{\text{SiCH}} = 4$ Hz, $^1J_{\text{SiH}} = 35$ Hz, H–Si); $^{31}\text{P}\{^1\text{H}\}\text{-NMR}$: $\delta = 23.04$ (s, with satellites, $^1J_{\text{PtP}} = 2850$ Hz, **3a**), 15.23 (s, with satellites, $^1J_{\text{PtP}} = 2089$ Hz, **1**), 14.91 (s, with satellites, $^1J_{\text{PtP}} = 2208$ Hz, **2**), –15.12 (s, de-coordinated P, N ligand); $^{29}\text{Si-NMR}$: $\delta = 15.7$ (Si–Pt), 6.6 (MeSiEt₃), 0.05 (HSiEt₃);

4.3. Reaction of $[(\kappa^2\text{-P,N})\text{-Me}_2\text{N}(\text{CH}_2)_3\text{PPh}_2]\text{PtMe}_2$ (**1**) with HSiPh₂Me

1:1 molar ratio: 4 mg (0.002 mmol) of HSiPh₂Me was added at r.t. to 10 mg (0.002 mmol) of **1** in 0.5 ml of C₆D₆. On addition of the silane no sign of reaction was observed. However, with increasing reaction time at r.t., the sample turned yellow, then orange and after 24 h

was dark brown, and a brown solid was present. After 24 h at r.t. the sample was heated for 60 min at 60 °C.

Excess of silane: 80 mg (0.48 mmol) of HSiPh₂Me was added at r.t. to 10 mg (0.002 mmol) of **1** in 0.4 ml of C₆D₆. On addition of the silane, the sample immediately turned yellow. With increasing reaction time the sample became darker, and a brown solid was present. After 5 h at r.t. the sample was heated for 90 min, and NMR spectra were taken.

$^1\text{H-NMR}$: $\delta = -18.9$ (d with satellites, $^2J_{\text{PH}} = 17$ Hz, $^1J_{\text{PtH}} = 1482$ Hz, **2**), 4.94 (q, with satellites, $^2J(\text{SiCH}) = 4\text{Hz}$, $^1J_{\text{SiH}} = 41$ Hz, H–Si); $^{31}\text{P}\{^1\text{H}\}\text{-NMR}$: $\delta = 28.23$ (d, with satellites, $^2J_{\text{SiPtP}} = 10.7$ Hz, $^1J_{\text{PtP}} = 1597$ Hz, **4**), 24.17 (d, with satellites, $^2J_{\text{SiPtP}} = 10.7$ Hz, $^1J_{\text{PtP}} = 2494$ Hz, **3b**), 15.23 (s, with satellites, $^1J_{\text{PtP}} = 2089$ Hz, **1**), 14.91 (s, with satellites, $^1J_{\text{PtP}} = 2170$ Hz, **2**); $^{29}\text{Si-NMR}$: $\delta = -7.97$ (s, MeSiPh₂Me), –10.6 (s, Si–Pt, **3b**), –17.7 (s, HSiMePh₂), –21.6 (s, Si–Pt, **4**); $^{195}\text{Pt-NMR}$: $\delta = -4790$ (d, $^1J_{\text{PtP}} = 2260$ Hz, **3b**), –4412 (d, $^1J_{\text{PtP}} = 2164$ Hz, **4**), –4073 (d, $^1J_{\text{PtP}} = 2056$ Hz, **1**).

4.4. X-ray structure analyses of **1** and **8**

Data collection (Table 3): the crystals were mounted on a Siemens SMART diffractometer (area detector). Mo–K α radiation ($\lambda = 71.069$ pm, graphite monochromator) was used for all measurements. The cell dimensions were refined with all unique reflections. The data collection (at 293 K) covered a hemisphere of the reciprocal space, by a combination of three sets of exposures. Each set had a different ϕ angle for the crystal, and each exposure took 20 s and covered 0.3° in ω . The crystal-to-detector distance was 4.40 cm. The reflections were corrected for polarization and Lorentz effects, and an empirical absorption correction (SADABS) was employed.

The structure was solved by direct methods (SHELXS-97). The positions of the hydrogen atoms were calculated according to an idealized geometry. Refinement was performed by the full-matrix least-squares method based on F^2 (SHELXL-97) with anisotropic thermal

Table 3
Crystallographic and structural parameters of **1** and **8**

	1 ·C ₆ H ₆	8
Empirical formula	C ₂₅ H ₂₂ NPPt	C ₂₂ H ₃₄ NPPt
Formula weight	562.5	538.6
Space group	<i>P</i> 2 ₁ / <i>n</i>	<i>P</i> 2 ₁ / <i>c</i>
Unit cell dimensions		
<i>a</i> (pm)	1595.1(2)	1134.2(5)
<i>b</i> (pm)	938.29 (9)	845.4(3)
<i>c</i> (pm)	1764.2 (2)	2293.6(9)
β (°)	112.959(2)	90.14(3)
<i>V</i> (pm ³)	2431.2(4) × 10 ⁶	2199(2) × 10 ⁶
<i>Z</i>	4	4
<i>D</i> _{calc} (g cm ⁻³)	1.537	1.627
μ (mm ⁻¹)	5.846	6.458
Crystal size (mm ³)	0.6 × 0.4 × 0.08	0.50 × 0.18 × 0.05
θ Range (°)	2.20–23.26	2.52–26.39
Reflections collected/unique	10912/3499	9877/3785
Data/parameters	3499/281	3785/228
GOF	1.089	1.084
<i>R</i> ₁ [<i>I</i> > 2σ(<i>I</i>)]	0.058	0.044
<i>wR</i> ₂	0.150	0.113
Largest difference peak and hole (e Å ⁻³)	2.229/–1.847	1.938/–1.517

parameters for all non-hydrogen atoms. The parameters of the hydrogen atoms were refined with a riding model.

5. Supplementary material

Crystallographic data (excluding structure factors) for the structural analysis have been deposited with the Cambridge Crystallographic Data Centre, CCDC nos. 207246 and 207245 compounds **1** and **8**, respectively. Copies of this information may be obtained free of charge from The Director, CCDC, 12 Union Road, Cambridge CB2 1EZ, UK (Fax: +44-1223-336033; e-mail: deposit@ccdc.cam.ac.uk or www: http://www.ccdc.cam.ac.uk).

Acknowledgements

This work was supported by the Fonds zur Förderung der wissenschaftlichen Forschung (FWF), Austria.

References

- [1] Account on previous work: U. Schubert, J. Pfeiffer, F. Stöhr, D. Sturmayer, S. Thompson, *J. Organomet. Chem.* 646 (2002) 53.
- [2] F. Stöhr, D. Sturmayer, G. Kickelbick, U. Schubert, *Eur. J. Inorg. Chem.* (2002) 2305.
- [3] J. Pfeiffer, G. Kickelbick, U. Schubert, *Organometallics* 19 (2000) 957.
- [4] F. Stöhr, D. Sturmayer, U. Schubert, *J. Chem. Soc. Chem. Commun.* (2002) 2222.
- [5] J. Pfeiffer, U. Schubert, *Organometallics* 18 (1999) 3245.
- [6] J. Pfeiffer, G. Kickelbick, U. Schubert, *Organometallics* 19 (2000) 62.
- [7] For example see: M.E. van der Boom, J. Ott, D. Milstein, *Organometallics* 17 (1998) 4263.
- [8] A word of caution should be given to the percentage values stated here. The hetero-nuclear spectra cannot be accurately integrated due to the method used, thus the values here are only quantitative estimates to give a general trend.
- [9] D. Sturmayer, U. Schubert, *Monatsh. Chem.* 134 (2003) 791.
- [10] H. Gilges, U. Schubert, *Organometallics* 17 (1998) 4760.
- [11] (a) For example: M.D. Curtis, P.S. Epstein, *Adv. Organomet. Chem.* 19 (1981) 213;
(b) L.S. Chang, M.P. Johnson, M. Fink, *Organometallics* 10 (1991) 1219;
(c) H. Yamashita, M. Tanaka, M. Goto, *Organometallics* 11 (1992) 3227;
(d) D.C. Pestana, T.S. Koloski, D.H. Berry, *Organometallics* 13 (1994) 4173;
(e) L.K. Figge, P.J. Carroll, D.H. Berry, *Organometallics* 15 (1996) 209;
(f) R.S. Simons, J.C. Gallucci, C.A. Tessier, W.J. Youngs, *J. Organomet. Chem.* 654 (2002) 224.
- [12] G.P. Mitchell, T.D. Tilley, *Angew. Chem. Int. Ed. Engl.* 39 (1998) 2524.
- [13] S.M. Thompson, U. Schubert, *Inorg. Chim. Acta* 350 (2003) 329.
- [14] M. Aizenberg, D. Milstein, *J. Am. Chem. Soc.* 117 (1995) 6456.
- [15] A.D. Sadow, T.D. Tilley, *Angew. Chem.* 115 (2003) 827; *Angew. Chem. Int. Ed. Engl.* 42 (2003) 807.
- [16] A.D. Becke, *J. Chem. Phys.* 18 (1993) 5648.
- [17] C. Lee, W. Yang, R.G. Parr, *Phys. Rev. B* 37 (1988) 785.
- [18] M.J. Frisch, G.W. Trucks, H.B. Schlegel, G.E. Scuseria, M.A. Robb, J.R. Cheeseman, V.G. Zakrzewski, J.A. Montgomery, R.E. Stratmann, J.C. Burant, S. Dapprich, J.M. Millam, A.D. Daniels, K.N. Kudin, M.C. Strain, O. Farkas, J. Tomasi, V. Barone, M. Cossi, R. Cammi, B. Mennucci, C. Pomelli, C. Adamo, S. Clifford, J. Ochterski, G.A. Petersson, P.Y. Ayala, Q. Cui, K. Morokuma, D.K. Malick, A.D. Rabuck, K. Raghavachari, J.B. Foresman, J. Cioslowski, J.V. Ortiz, B.B. Stefanov, G. Liu, A. Liashenko, P. Piskorz, I. Komaromi, R. Gomperts, R.L. Martin, D.J. Fox, T. Keith, M.A. Al-Laham, C.Y. Peng, A. Nanayakkara, C. Gonzalez, M. Challacombe, P.M.W. Gill, B. Johnson, W. Chen, M.W. Wong, J.L. Andres, C. Gonzalez, M. Head-Gordon, E.S. Replogle, J.A. Pople Gaussian, Inc., Pittsburgh, PA, 1998.